Low-momentum NN interactions and all-order summation of ring diagrams of symmetric nuclear matter

L.-W. Siu, J. W. Holt, T. T. S. Kuo,* and G. E. Brown
Department of Physics and Astronomy, Stony Brook University, New York 11794-3800, USA
(Received 26 November 2008; revised manuscript received 13 April 2009; published 13 May 2009)

We study the equation of state for symmetric nuclear matter using a ring-diagram approach in which the particle-particle hole-hole (pphh) ring diagrams within a momentum model space of decimation scale Λ are summed to all orders. The calculation is carried out using the renormalized low-momentum nucleon-nucleon (NN) interaction $V_{\text{low-}k}$, which is obtained from a bare NN potential by integrating out the high-momentum components beyond Λ. The bare NN potentials of CD-Bonn, Nijmegen, and Idaho have been employed. The choice of Λ and its influence on the single particle spectrum are discussed. Ring-diagram correlations at intermediate momenta ($k \simeq 2$ fm^{-1}) are found to be particularly important for nuclear saturation, suggesting the necessity of using a sufficiently large decimation scale so that the above momentum region is not integrated out. Using $V_{\text{low-}k}$ with $\Lambda \sim 3$ fm^{-1}, we perform a ring-diagram computation with the above potentials, which all yield saturation energies E/A and Fermi momenta $k_F^{(0)}$ considerably larger than the empirical values. On the other hand, similar computations with the medium-dependent Brown-Rho scaled NN potentials give satisfactory results of $E/A \simeq -15$ MeV and $k_F^{(0)} \simeq 1.4$ fm^{-1}. The effect of this medium dependence is well reproduced by an empirical three-body force of the Skyrme type.

DOI: 10.1103/PhysRevC.79.054004 PACS number(s): 21.30.−x, 21.65.Mn, 21.45.Ff

I. INTRODUCTION

Obtaining the energy per nucleon (E/A) as a function of the Fermi momentum (k_F) for symmetric nuclear matter is one of the most important problems in nuclear physics. Empirically, nuclear matter saturates at $E/A \simeq -16$ MeV and $k_F \simeq 1.36$ fm^{-1}. A great amount of effort has been put into computing the above quantities starting from a microscopic many-body theory. For many years, the Brueckner-Hartree-Fock (BHF) theory [1–3] was the primary framework for nuclear matter calculations. However, BHF represents only the first-order approximation in the general hole-line expansion [4]. Conclusive studies [5–7] have shown that the hole-line expansion converges at the third order (or the second order with a continuous single-particle spectrum) and that such results are in good agreement with variational calculations [8] of the binding energy per nucleon. Nonetheless, all such calculations have shown that it is very difficult to obtain *both* the empirical saturation energy and the saturation Fermi momentum simultaneously. In fact, such calculations using various models of the nucleon-nucleon interaction result in a series of saturation points that actually lie along a band, often referred to as the Coester band [9], which deviates significantly from the empirical saturation point. For this reason it is now widely believed that free-space two-nucleon interactions alone are insufficient to describe the properties of nuclear systems close to saturation density and that accurate results can only be achieved by introducing higher-order effects, e.g., three-nucleon forces [10] or relativistic effects [11].

In the present work, we carry out calculations of the nuclear binding energy for symmetric nuclear matter using a framework based on a combination of the recently developed low-momentum NN interaction $V_{\text{low-}k}$ [12–17] and the ring-diagram method for nuclear matter of Song, Yang, and Kuo [18], which is a model-space approach where the particle-particle hole-hole (pphh) ring diagrams for the potential energy of nuclear matter are summed to all orders. In previous studies a model space of size $\Lambda \sim 3$ fm^{-1} was used to obtain improved results compared with those from the BHF method. Such an improvement can be attributed to the following desirable features in the ring-diagram approach. First, the ground-state energy shift ΔE_0 in the BHF approach is given by just the lowest-order reaction matrix (G matrix) diagram (corresponding to Fig. 1(b) with the dashed vertex representing G). It does not include diagrams corresponding to the particle-hole excitations of the Fermi sea. Such excitations represent the effect of long-range correlations. In contrast, the pphh ring diagrams, such as those in Figs. 1(c) and 1(d), are included to all orders in the ring-diagram approach. Second, the single-particle (s.p.) spectrum used in the ring-diagram approach is different from that in early BHF calculations, where one typically employed a self-consistent s.p. spectrum for momenta $k \leqslant k_F$ and a free-particle spectrum otherwise. Thus the s.p. spectrum had a large artificial discontinuity at k_F. The s.p. spectrum used in the ring-diagram approach is a continuous one. The importance of using a continuous s.p. spectrum in nuclear matter theory has been discussed and emphasized in Refs. [6] and [7]. Within the above ring-diagram framework, previous calculations [19] using G-matrix effective interactions and $\Lambda \sim 3$ fm^{-1} have yielded saturated nuclear matter that is slightly overbound ($E/A \simeq -18$ MeV) and that saturates at too high a density ($k_F \simeq 1.6$ fm^{-1}) compared to empirical data. These results are consistent, within theoretical errors, with calculations based on the third-order hole-line expansion and variational methods (see Refs. [5,6,8]).

*thomas.kuo@stonybrook.edu

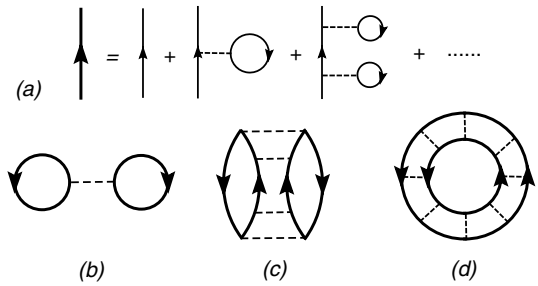

FIG. 1. Diagrams included in the pphh ring-diagram summation for the ground-state energy shift of symmetric nuclear matter. Included are (a) self-energy insertions on the single-particle propagator and (b)–(d) pphh correlations.

In the past, the above ring-diagram approach [18,19] employed the G-matrix interaction, which is energy dependent, meaning that the whole calculation must be done in a "self-consistent" way. The calculation would be greatly simplified if this energy dependence, and thus the self-consistency procedure, were removed. Such an improvement has occurred in the past several years with the development of a low-momentum NN interaction, $V_{\text{low-}k}$, constructed from renormalization group techniques [12–17]. As discussed in these references, the $V_{\text{low-}k}$ interaction has a number of desirable properties, such as being nearly unique as well as being a smooth potential suitable for perturbative many-body calculations [20]. Furthermore, $V_{\text{low-}k}$ is energy independent, making it a convenient choice for the interaction used in ring-diagram calculations of nuclear matter.

The $V_{\text{low-}k}$ interaction has been extensively used in nuclear shell-model calculations for nuclei with a few valence nucleons outside a closed shell. As reviewed recently by Coraggio *et al.* [21], the results obtained from such shell-model calculations are in very good agreement with experiments. However, applications of the $V_{\text{low-}k}$ interaction to nuclear matter have been relatively few [20,22–24]. A main purpose of the present work is to study the suitability of describing symmetric nuclear matter using $V_{\text{low-}k}$. A concern about such applications is that the use of $V_{\text{low-}k}$ alone may not provide satisfactory nuclear saturation. As illustrated in Ref. [22], Hartree-Fock (HF) calculations of nuclear matter using $V_{\text{low-}k}$ with a cutoff momentum of $\Lambda \sim 2.0$ fm^{-1} do not yield nuclear saturation—the calculated E/A decreases monotonically with k_F up to the decimation scale Λ.

In this work, we carry out a ring-diagram calculation of symmetric nuclear matter with $V_{\text{low-}k}$. We show in detail that satisfactory results for the saturation energy and saturation Fermi momentum can be obtained when one takes into account the following two factors: a suitable choice of the cutoff momentum and the in-medium modification of meson masses. As we discuss, ring-diagram correlations at intermediate momenta ($k \sim 2.0$ fm^{-1}) have strong medium dependence and are important for nuclear saturation. To include their effects one needs to use a sufficiently large decimation scale Λ so that the above momentum range is not integrated out. We have carried out ring-diagram calculations for symmetric nuclear matter using $\Lambda \sim 3$ fm^{-1} with several modern high-precision NN potentials, and the results yield nuclear saturation. However, E/A and k_F at saturation are both considerably larger in magnitude than the corresponding empirical values. Great improvement can be obtained when one takes into account medium modifications to the exchanged mesons. Clearly mesons in a nuclear medium and those in free space are different: the former are "dressed" while the latter are "bare." Brown and Rho have suggested that the dependence of meson masses on nuclear density can be described by a simple equation known as Brown-Rho scaling [25,26]:

$$\sqrt{\frac{g_A}{g_A^*}}\frac{m_N^*}{m_N} = \frac{m_\sigma^*}{m_\sigma} = \frac{m_\rho^*}{m_\rho} = \frac{m_\omega^*}{m_\omega} = \frac{f_\pi^*}{f_\pi} = \Phi(n), \qquad (1)$$

where g_A is the axial coupling constant, Φ is a function of the nuclear density n, and the star indicates in-medium values of the given quantities. At saturation density, $\Phi(n_0) \simeq 0.8$. In a high-density medium such as nuclear matter, these medium modifications of meson masses are significant and can render V_{NN} quite different from that in free space. Thus, in contrast to shell-model calculations for nuclei with only a few valence particles, for nuclear matter calculations it may be necessary to use a V_{NN} with medium modifications *built in*. In the present work, we carry out such a ring-diagram summation using a Brown-Rho scaled NN interaction.

The Skyrme [27] interaction is one of the most successful effective nuclear potentials. An important component of this interaction is a zero-range three-body force, which is equivalent to a density-dependent two-body force. Note that the importance of three-body interactions in achieving nuclear saturation with low-momentum interactions has been extensively discussed in the literature (see Ref. [20] and references quoted therein). In the last part of our work, we study whether the density dependence from Brown-Rho scaling can be well represented by that from an empirical density-dependent force of the Skyrme type.

The organization of this article is as follows. In Secs. II and III we outline our model-space pphh ring-diagram calculation for the nuclear binding energy and the concept of Brown-Rho scaling, respectively. In Sec. IV we present our computational results. A brief conclusion can be found in Sec. V.

II. SUMMATION OF pphh RING DIAGRAMS

In this section we describe how to calculate the properties of symmetric matter using the low-momentum ring-diagram method. We employ a momentum model space where all nucleons have momenta $k \leqslant \Lambda$. By integrating out the $k > \Lambda$ components, the low-momentum interaction $V_{\text{low-}k}$ is constructed for summing the pphh ring diagrams within the model space.

The ground-state energy shift $\Delta E_0 = E_0 - E_0^{\text{free}}$ for nuclear matter is defined as the difference between the true ground-state energy E_0 and the corresponding quantity for the noninteracting system E_0^{free}. In the present work, we consider ΔE_0 as given by the all-order sum of the pphh ring diagrams as shown in Figs. 1(b)–1(d).

We shall calculate the all-order sum, denoted as ΔE_0^{pp}, of such diagrams. Each vertex in a ring diagram is the renormalized effective interaction $V_{\text{low-}k}$ corresponding to the

model space $k \leqslant \Lambda$. It is obtained from the following T-matrix equivalence method [12–17]. Let us start with the T-matrix equation

$$T(k', k, k^2) = V(k', k) + \mathcal{P}\int_0^\infty q^2 dq \frac{V(k', q)T(q, k, k^2)}{k^2 - q^2}, \quad (2)$$

where V is a bare NN potential. In the present work we use the CD-Bonn [28], Nijmegen-I [29], and Idaho (chiral) [30] NN potentials. Notice that in the above equation the intermediate-state momentum q is integrated from 0 to ∞. We then define an effective low-momentum T-matrix by

$$T_{\text{low-}k}(p', p, p^2) = V_{\text{low-}k}(p', p) + \mathcal{P}\int_0^\Lambda q^2 dq \times \frac{V_{\text{low-}k}(p', q)T_{\text{low-}k}(q, p, p^2)}{p^2 - q^2}, \quad (3)$$

where the intermediate-state momentum is integrated from 0 to Λ, the momentum space cutoff. The low-momentum interaction $V_{\text{low-}k}$ is then obtained from the above equations by requiring the T-matrix equivalence condition to hold, namely,

$$T(p', p, p^2) = T_{\text{low-}k}(p', p, p^2); \quad (p', p) \leqslant \Lambda. \quad (4)$$

The iteration method of Lee-Suzuki-Andreozzi [17,31,32] has been used in obtaining the above $V_{\text{low-}k}$.

With $V_{\text{low-}k}$, our ring-diagram calculations are relatively simple, compared to the G-matrix calculations of Ref. [18]. Within the model space, we use the Hartree-Fock s.p. spectrum calculated with the $V_{\text{low-}k}$ interaction, and outside the model space we use the free particle spectrum. In other words,

$$\epsilon_k = \begin{cases} \hbar^2k^2/2m + \sum_{h<k_F}\langle kh|V_{\text{low-}k}|kh\rangle; & k \leqslant \Lambda \\ \hbar^2k^2/2m; & k > \Lambda. \end{cases} \quad (5)$$

The above s.p. spectrum is medium (k_F) dependent.

Our next step is to solve the model-space RPA equation

$$\sum_{ef}[(\epsilon_i + \epsilon_j)\delta_{ij,ef} + \lambda(\bar{n}_i\bar{n}_j - n_in_j)\langle ij|V_{\text{low-}k}|ef\rangle]Y_n(ef, \lambda) = \omega_n Y_n(ij, \lambda); (i, j, e, f) \leqslant \Lambda, \quad (6)$$

where $n_a = 1$ for $a \leqslant k_F$ and $n_a = 0$ for $a > k_F$; also $\bar{n}_a = (1 - n_a)$. The strength parameter λ is introduced for calculational convenience and varies between 0 and 1. Note that the above equation is within the model space as indicated by $(i, j, e, f) \leqslant \Lambda$. The transition amplitudes Y of the above equation can be classified into two types, one dominated by hole-hole components and the other by particle-particle components. We use only the former, denoted by Y_m, for the calculation of the all-order sum of the pphh ring diagrams. This sum is given by [18,24,33]

$$\Delta E_0^{\text{pp}} = \int_0^1 d\lambda \sum_m \sum_{ijkl<\Lambda} Y_m(ij, \lambda) \times Y_m^*(kl, \lambda)\langle ij|V_{\text{low-}k}|kl\rangle, \quad (7)$$

where the normalization condition for Y_m is $\langle Y_m|\frac{1}{Q}|Y_m\rangle = -1$ and $Q(i, j) = (\bar{n}_i\bar{n}_j - n_in_j)$. In the above, Σ_m means we sum over only those solutions of the RPA equation (6) that are dominated by hole-hole components as indicated by the normalization condition.

The all-order sum of the pphh ring diagrams as indicated by Figs. 1(b)–1(d) is given by the above ΔE_0^{pp}. Because we use the HF s.p. spectrum, each propagator of the diagrams contains the HF insertions to all orders as indicated by Fig. 1(a). Clearly our ring diagrams are medium dependent; their s.p. propagators have all-order HF insertions that are medium dependent, as is the occupation factor $(\bar{n}_i\bar{n}_j - n_in_j)$ of the RPA equation.

III. BROWN-RHO SCALING AND IN-MEDIUM NN INTERACTIONS

Nucleon-nucleon interactions are mediated by meson exchange, and clearly the in-medium modification of meson masses is important for NN interactions. These modifications could arise from the partial restoration of chiral symmetry at finite density/temperature or from traditional many-body effects. Particularly important are the vector mesons, for which there is now evidence from both theory [34–36] and experiment [37,38] that the masses may decrease by approximately 10–15% at normal nuclear matter density and zero temperature. This in-medium decrease of meson masses is often referred to as Brown-Rho scaling [25,26]. For densities below that of nuclear matter, it is suggested [34] that the masses decrease linearly with the density n:

$$\frac{m_V^*}{m_V} = 1 - C\frac{n}{n_0}, \quad (8)$$

where m_V^* is the vector meson mass in-medium, n_0 is nuclear matter saturation density, and C is a constant of value $\sim$0.10–0.15.

We study the consequences for nuclear many-body calculations by replacing the NN interaction in free space with a density-dependent interaction with medium-modified meson exchange. A simple way to obtain such potentials is by modifying the meson masses and relevant parameters of the one-boson-exchange NN potentials (e.g., the Bonn and Nijmegen interactions). The saturation of nuclear matter is an appropriate phenomenon for studying the effects of dropping masses [23,39], because the density of nuclear matter is constant and large enough to significantly affect the nuclear interaction through the modified meson masses.

One unambiguous prediction of Brown-Rho scaling in dense nuclear matter is the decreasing of the tensor force component of the nuclear interaction. The two most important contributions to the tensor force come from π and ρ meson exchange, which act opposite to each other:

$$V_\rho^T(r) = -\frac{f_\rho^2}{4\pi}m_\rho\tau_1 \cdot \tau_2 S_{12} f_3(m_\rho r), \quad (9)$$

$$V_\pi^T(r) = \frac{f_\pi^2}{4\pi}m_\pi\tau_1 \cdot \tau_2 S_{12} f_3(m_\pi r), \quad (10)$$

$$f_3(mr) = \left(\frac{1}{(mr)^3} + \frac{1}{(mr)^2} + \frac{1}{3mr}\right)e^{-mr}. \quad (11)$$

In Brown-Rho scaling the ρ meson is expected to decrease in mass at finite density while the pion mass remains nearly

unchanged due to chiral invariance. Therefore, the overall strength of the tensor force at finite density will be significantly smaller than that in free space. As we shall discuss later, this decrease in the tensor force plays an important role for nuclear saturation.

The Skyrme effective interaction has been widely used in nuclear physics and has been very successful in describing the properties of finite nuclei as well as nuclear matter [27]. This interaction has both two-body and three-body terms, having the form

$$V_{\text{skyrme}} = \sum_{i<j} V(i,j) + \sum_{i<j<k} V(i,j,k). \tag{12}$$

Here $V(i,j)$ is a momentum ($\vec{k}$)-dependent zero-range interaction, containing two types of terms: one with no momentum dependence and the other depending quadratically on $\vec{k}$. $V(i,j)$ corresponds to a low-momentum expansion of an underlying NN interaction. Its three-body term is a zero-range interaction,

$$V(i,j,k) = t_3\delta(\vec{r}_i - \vec{r}_j)\delta(\vec{r}_j - \vec{r}_k), \tag{13}$$

which is equivalent to a density-dependent two-body interaction of the form

$$V_\rho(1,2) = \tfrac{1}{6}t_3\delta(\vec{r}_1 - \vec{r}_2)\rho(\vec{r}_{\text{av}}), \tag{14}$$

with $\vec{r}_{\text{av}} = \frac{1}{2}(\vec{r}_1 + \vec{r}_2)$.

The general structure of V_{skyrme} is rather similar to the effective interactions based on effective field theories (EFT) [20], with $V(i,j)$ corresponding to $V_{\text{low-}k}$ and $V(i,j,k)$ to the EFT three-body force. The Skyrme three-body force, however, is much simpler than that in EFT. We compare in the next section the density-dependent effect generated by the medium modified NN interaction with that from an empirical three-body force of the Skyrme type.

IV. RESULTS AND DISCUSSIONS

In this section, we report computational results for the binding energy of symmetric nuclear matter calculated with an all-order summation of low-momentum pphh ring diagrams. The method is already outlined and discussed in the above sections. As mentioned above, we employ a model-space approach. Starting from various bare NN interactions, we first construct the low-momentum interactions $V_{\text{low-}k}$ with a particular choice of the cutoff momentum Λ. The low-momentum ($<\Lambda$) pphh ring diagrams are then summed to all orders as given by Eq. (7) to give the binding energy.

A. Single-particle spectrum and nuclear binding energy

First, we look carefully into the role of Λ in our ring-diagram calculation. Let us start with the s.p. energy ϵ_k. Obtaining ϵ_k is the first step in our ring-diagram calculation. Within our model-space approach, ϵ_k is given by the Hartree-Fock spectrum for $k \leqslant \Lambda$, while for $k > \Lambda$, ϵ_k is taken as the free spectrum [see Eq. (5)]. As emphasized before, the s.p. spectrum obtained in this way will in general have a discontinuity at Λ. Such a discontinuity is a direct consequence of having a finite model space. It is of much interest to study the s.p. spectrum as Λ is varied. In Fig. 2, we plot the spectrum for different values of Λ ranging from 2 to 4 fm^{-1}. We observed that with $\Lambda = 2.0$ fm^{-1}, the discontinuity at Λ is relatively large; there is a gap of about 50 MeV between the s.p. spectrum just inside Λ and that outside. However, this discontinuity decreases if Λ is increased to around 3 fm^{-1}. At this point, the s.p. spectrum is most "satisfactory" in the sense of being almost continuous. A further increase in Λ will result in an "unreasonable" situation where the s.p. spectrum just inside Λ becomes significantly higher than that outside. This is clearly shown in the data of $\Lambda = 4.0$ fm^{-1}. The above results suggest that to have a nearly continuous s.p. spectrum, which is physically desirable, it is necessary to use $\Lambda \sim 3$ fm^{-1}.

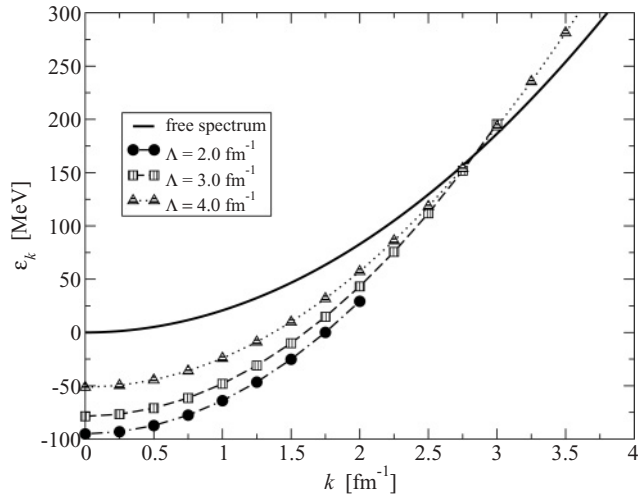

FIG. 2. Dependence of the model-space s.p. spectrum on the decimation scale Λ for symmetric nuclear matter at the empirical saturation density. The CD-Bonn potential is used in the construction of $V_{\text{low-}k}$.

Next, we look into the effect of Λ on the nuclear binding energy. Once the s.p. energies are obtained, the all-order ring-diagram summation can be carried out [see Eqs. (6) and (7)]. Let us first discuss the computational results based on the CD-Bonn potential. Results from various Λ ranging from 2 to 3.2 fm^{-1} are shown in Fig. 3. Let us focus on (i) the overall saturation phenomena and (ii) the numerical values of the binding energy and the saturation momentum.

(i) We observe that the nuclear binding energy exhibits saturation only when Λ is $\sim$3 fm^{-1} and beyond. This reflects the importance of ring diagrams in the intermediate-momentum region ($k \sim 2$ fm^{-1}). To illustrate, let us compare the results for the cases of $\Lambda = 2$ and 3 fm^{-1}. As indicated by Eqs. (2)–(4), $V_{\text{low-}k}$ includes only the $k > \Lambda$ pp ladder interactions between a pair of "free" nucleons; there is no medium correction included. Thus the above two cases treat correlations in the momentum region between 2 and 3 fm^{-1} differently: the former includes for this momentum region only pp ladder interactions with medium effect neglected, while the latter includes both pp and hh correlations with medium effect, such as that from the Pauli blocking, included. Our results

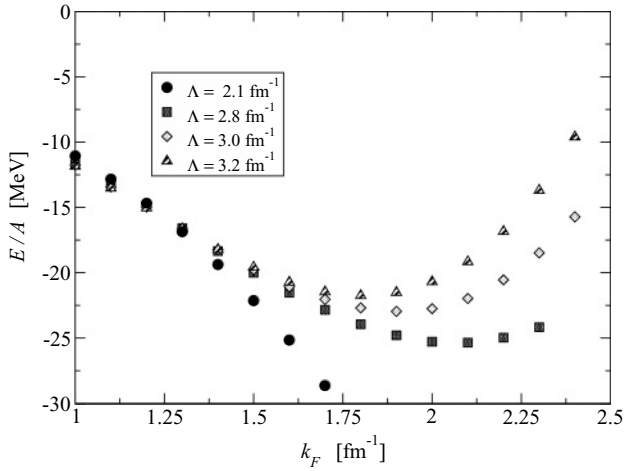

FIG. 3. Results for the energy per nucleon (E/A) of symmetric nuclear matter obtained by summing up the pphh ring diagrams to all orders. Low-momentum NN interactions, constructed from the CD-Bonn potential, with various cutoffs Λ are used in the ring-diagram summation.

indicate that the medium effect in the above momentum region is vital for saturation.

For nuclear matter binding energy calculations, there is no first-order contribution from the tensor force (V_T); its leading contribution is second order of the form $\langle {}^3S_1|V_T\frac{Q}{e}V_T|{}^3S_1\rangle$, where Q stands for the Pauli blocking operator and e the energy denominator. Thus the contribution from the tensor force depends largely on the availability of the intermediate states; this contribution is large for low k_F but is suppressed for high k_F. To illustrate this point, we plot the potential energy of nuclear matter from the ${}^1S_0$ and ${}^3S_1 - {}^3D_1$ channels separately in Fig. 4. The behavior of the potential energy in these two channels differ in a significant way. The ${}^1S_0$ channel is practically independent of the choice of Λ, as displayed in the upper panel of the figure. This indicates that for this channel the effects from medium corrections and hh correlations are not important. Also the PE/A from this channel does not exhibit saturation at a reasonable k_F. In the lower panel of the figure, we display the PE/A for the ${}^3S_1 - {}^3D_1$ channel where the tensor force is important. As seen, PE/A does not exhibit saturation when using $\Lambda = 2$ fm^{-1}. On the contrary, the result using $\Lambda = 3$ fm^{-1} shows a clear saturation behavior. This is mainly because in the former case the Pauli blocking effect is ignored for the momentum region 2–3 fm^{-1} while it is included for the latter. To have saturation, we should not integrate out the momentum components in the NN interaction that are crucial for saturation. Considering also the effect of Λ on the s.p. spectrum, we believe that $\Lambda = 3.0$ fm^{-1} is a suitable choice for our ring-diagram nuclear matter calculation. Notice that a model space $\sim$3 fm^{-1} has been used in other similar ring-summation calculations using G-matrix effective interactions [18,19].

(ii) We have performed a similar ring summation with the Nijmegen I and Idaho potentials. Results with $\Lambda = 3.0$ fm^{-1} are compared with those from CD-Bonn as shown in Fig. 5. The saturation energies for these three potentials are located between -19 and -23 MeV, while the saturation momentum ranges from 1.75 to 1.85 fm^{-1}. These quantities are considerably larger than the empirical values of -16 MeV and 1.4 fm^{-1}, respectively. We believe that improvements can be obtained if one takes into account the medium dependence of the NN interaction. Namely, instead of using a $V_{\text{low-}k}$ constructed from a bare NN interaction, one should employ a $V_{\text{low-}k}$ constructed from a "scaled" NN interaction according to the nuclear density. Below we report how we incorporate such effects into our ring-diagram summation.

B. Nuclear binding energy with Brown-Rho scaling

The concept of Brown-Rho scaling has already been discussed in Sec. III. The medium effects on the NN interaction resulting from the in-medium modification of meson masses

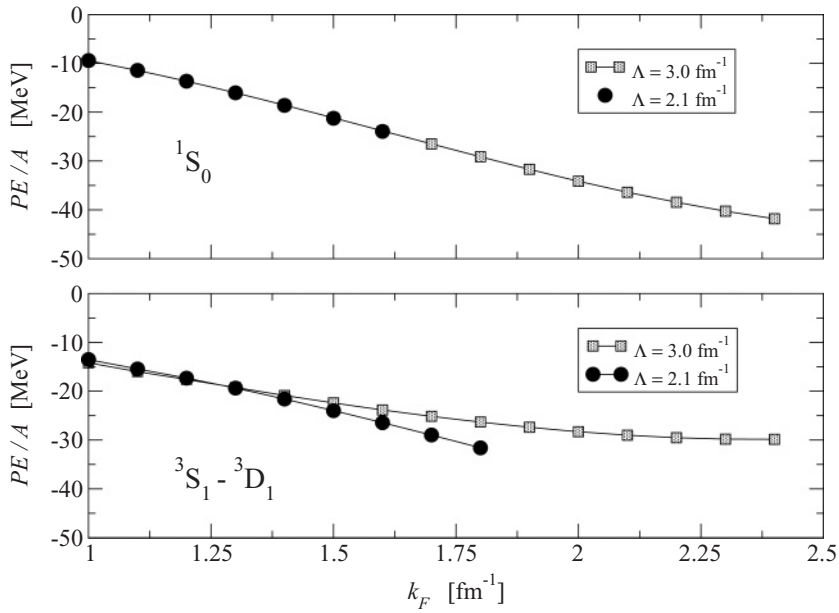

FIG. 4. Potential energy per nucleon (PE/A) in the ${}^1S_0$ and ${}^3S_1 - {}^3D_1$ channels of symmetric nuclear matter from summing up pphh ring diagrams to all orders. The CD-Bonn potential is used in the construction of $V_{\text{low-}k}$.

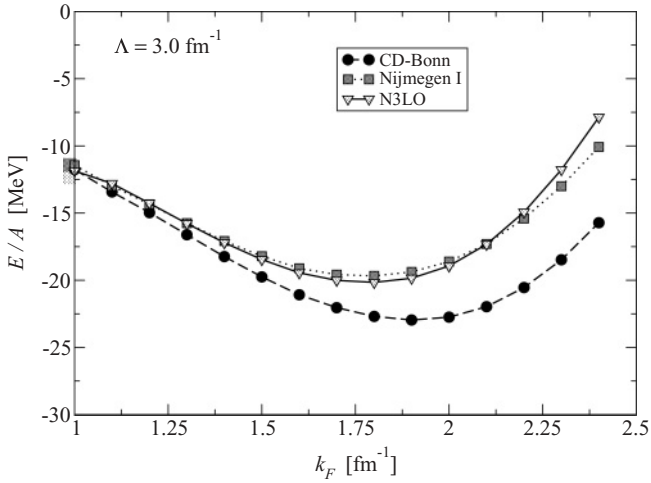

FIG. 5. The binding energy of symmetric nuclear matter from the low-momentum ring-diagram summation using various NN potentials. A momentum-space cutoff of $\Lambda = 3.0$ fm^{-1} is used.

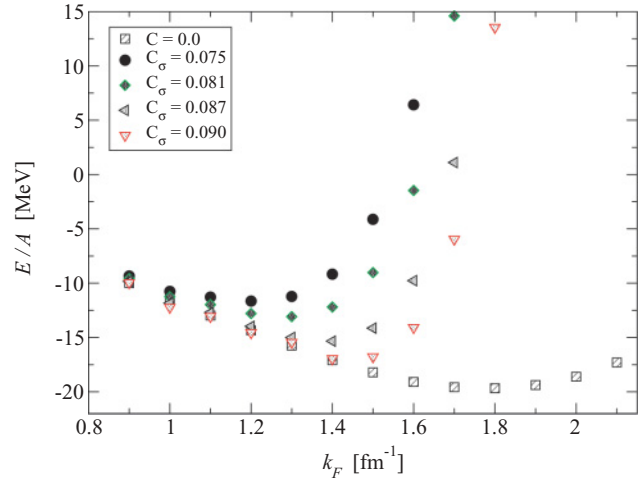

FIG. 6. (Color online) The binding energy of symmetric nuclear matter from the Brown-Rho scaled low-momentum Nijmegen II interaction using the ring-diagram summation with $\Lambda = 3.0$ fm^{-1}. Calculations for different choices of the σ meson scaling constant C_σ are shown.

have a profound effect on nuclear binding. To incorporate this in our ring-diagram calculation we work with the Nijmegen potential, which is one of the pure one-boson-exchange NN potentials. The bare Nijmegen is first Brown-Rho scaled [see Eq. (8)] with the dropping mass ratio C chosen to be 0.15. Vector meson masses in a nuclear medium have been widely studied both theoretically and experimentally, but the σ meson mass is not well constrained. Previous calculations [39] of nuclear matter saturation within the Dirac-Brueckner-Hartree-Fock formalism showed that there is too much attraction when the σ meson is scaled according to Eq. (8). However, a microscopic treatment [39] of σ meson exchange in terms of correlated 2π exchange showed that the medium effects on the σ are much weaker than those in Eq. (8). Therefore, in our ring-diagram summation using the Brown-Rho scaled Nijmegen II interaction, we employ a range of scaling parameters C_σ between 0.075 and 0.09. Our calculations are shown in Fig. 6. With Brown-Rho scaling, the numerical values for both the saturation energy and saturation momentum are greatly improved. Whereas the unscaled potential gives a binding energy BE/$A \simeq 20$ MeV and $k_F^0 \simeq 1.8$ fm^{-1}, the scaled potential gives BE/$A \simeq 14$–17 MeV and $k_F^0 \simeq 1.30$–1.45 fm^{-1} for a σ meson scaling constant $C_\sigma \sim 0.08$–0.09, in very good agreement with the empirical values.We conclude, first, that the medium dependence of nuclear interactions is crucial for a satisfactory description of nuclear saturation and, second, that within the framework of one-boson-exchange NN interaction models one can obtain an adequate description of nuclear matter saturation by including Brown-Rho scaled meson masses.

C. Nuclear binding energy with three-body force of the Skyrme type

As discussed earlier in Sec. III, the widely used Skyrme interaction contains a three-body term that is equivalent to a density-dependent two-body interaction. It is of much interest to study whether our result with Brown-Rho scaled Nijmegen potential can be reproduced with the unscaled Nijmegen plus an effective three-body interaction of the Skyrme type that is characterized by a strength parameter, t_3 [see Eq. (14)]. In Fig. 7 we compare the results using $t_3 = 1250$ with our previous calculations using the Brown-Rho scaled Nijmegen II potential with a σ meson scaling constant of $C_\sigma = 0.087$. In all calculations $\Lambda = 3.0$ is used. We note that satisfactory results for the saturation energy and Fermi momentum are obtained using either Brown-Rho scaling or a 3NF of the Skyrme type. However, the nuclear incompressibility is considerably larger in the case of Brown-Rho scaling.

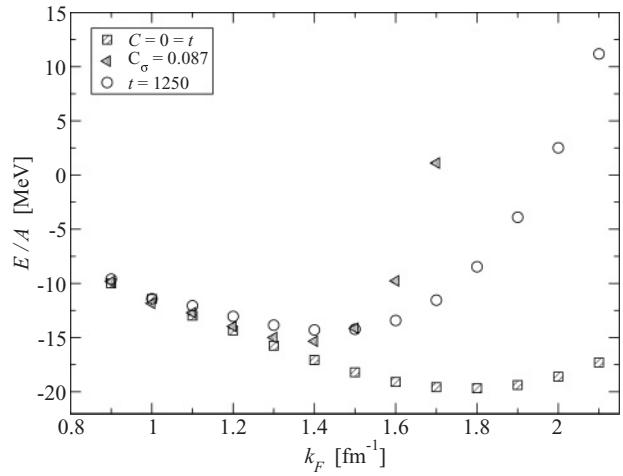

FIG. 7. The binding energy of symmetric nuclear matter from the low-momentum ring-diagram summation with $\Lambda = 3.0$ fm^{-1}. Three different interactions are used: (1) the medium-independent Nijmegen II interaction, the Brown-Rho scaled interaction with $C_\sigma = 0.087$, and finally the Nijmegen II interaction supplemented with a 3NF of the Skyrme type with $t_3 = 1250$.

V. CONCLUSION

We have studied the equation of state for symmetric nuclear matter using the low-momentum nucleon-nucleon (NN) interaction $V_{\text{low-}k}$. Particle-particle hole-hole (pphh) ring diagrams within a momentum model space $k < \Lambda$ were summed to all orders. The significant role of the intermediate-momentum range ($\sim$2.0 fm^{-1}) for nuclear saturation was discussed. We concluded that, in the ring-diagram summation, having a sufficiently large model space is important to capture the saturation effect from the intermediate-momentum components. Various bare NN potentials including CD-Bonn, Nijmegen, and Idaho have been employed, resulting in nuclear saturation with $\Lambda = 3.0$ fm^{-1}. However, the resulting binding energy and saturation momentum are still much larger than the empirical values. Improvement can be obtained when we take into account the medium modification of NN interaction. We first constructed $V_{\text{low-}k}$ from a medium-dependent Brown-Rho scaled NN potential and then implemented this into the ring-diagram summation. Satisfactory results of $E/A \simeq -15$ MeV and $k_F^{(0)} \simeq 1.4$ fm^{-1} could then be obtained. We showed that these saturation properties are well reproduced by the first ring-diagram approach with the addition of an empirical three-body force of the Skyrme type.

In the future, it is of much interest to carry out a BCS calculation on nuclear matter with $V_{\text{low-}k}$, particularly for the $^3S_1 - {}^3D_1$ channel where earlier calculations using bare NN interactions revealed a gap of 10 MeV around normal nuclear matter densities [40,41]. Recently, $V_{\text{low-}k}$ has been applied to obtain the equation of state of neutron matter [24,42] and the $^1S_0$ pairing gap [42,43]. A similar calculation on nuclear matter that incorporates the tensor correlations is obviously important and we plan to investigate it in the future.

ACKNOWLEDGMENTS

We thank R. Machleidt for many helpful discussions. This work was supported in part by US Department of Energy under Grant DF-FG02-88ER40388.

[1] H. A. Bethe, Annu. Rev. Nucl. Sci. **21**, 93 (1971).
[2] R. Machleidt, Adv. Nucl. Phys. **19**, 189 (1989).
[3] J. W. Holt and G. E. Brown, in *Hans Bethe and His Physics,* edited by G. E. Brown and C.-H. Lee (World Scientific, Singapore, 2006).
[4] B. D. Day, Rev. Mod. Phys. **50**, 495 (1978).
[5] B. D. Day, Phys. Rev. C **24**, 1203 (1981).
[6] H. Q. Song, M. Baldo, G. Giansiracusa, and U. Lombardo, Phys. Lett. **B411**, 237 (1997).
[7] H. Q. Song, M. Baldo, G. Giansiracusa, and U. Lombardo, Phys. Rev. Lett. **81**, 1584 (1998).
[8] B. D. Day and R. B. Wiringa, Phys. Rev. C **32**, 1057 (1985).
[9] F. Coester, S. Cohen, B. D. Day, and C. M. Vincent, Phys. Rev. C **1**, 769 (1970).
[10] R. B. Wiringa, V. Fiks, and A. Fabrocini, Phys. Rev. C **38**, 1010 (1988).
[11] R. Brockmann and R. Machleidt, Phys. Rev. C **42**, 1965 (1990).
[12] S. K. Bogner, T. T. S. Kuo, and L. Coraggio, Nucl. Phys. **A684**, 432 (2001).
[13] S. K. Bogner, T. T. S. Kuo, L. Coraggio, A. Covello, and N. Itaco, Phys. Rev. C **65**, 051301(R) (2002).
[14] L. Coraggio, A. Covello, A. Gargano, N. Itaco, T. T. S. Kuo, D. R. Entem, and R. Machleidt, Phys. Rev. C **66**, 021303(R) (2002).
[15] A. Schwenk, G. E. Brown, and B. Friman, Nucl. Phys. **A703**, 745 (2002).
[16] S. K. Bogner, T. T. S. Kuo, and A. Schwenk, Phys. Rep. **386**, 1 (2003).
[17] J. D. Holt, T. T. S. Kuo, and G. E. Brown, Phys. Rev. C **69**, 034329 (2004).
[18] H. Q. Song, S. D. Yang, and T. T. S. Kuo, Nucl. Phys. **A462**, 491 (1987).
[19] M. F. Jiang, T. T. S. Kuo, and H. Müther, Phys. Rev. C **38**, 2408 (1988).
[20] S. K. Bogner, A. Schwenk, R. J. Furnstahl, and A. Nogga, Nucl. Phys. **A763**, 59 (2005).
[21] L. Coraggio, A. Covello, A. Gargano, N. Itako, and T. T. S. Kuo, Prog. Part. Nucl. Phys. **62**, 135 (2009).
[22] J. Kuckei, F. Montani, H. Müther, and A. Sedrakian, Nucl. Phys. **A723**, 32 (2003).
[23] J. W. Holt, G. E. Brown, J. D. Holt, and T. T. S. Kuo, Nucl. Phys. **A785**, 322 (2007).
[24] L.-W. Siu, T. T. S. Kuo, and R. Machleidt, Phys. Rev. C **77**, 034001 (2008).
[25] G. E. Brown and M. Rho, Phys. Rev. Lett. **66**, 2720 (1991).
[26] G. E. Brown and M. Rho, Phys. Rep. **396**, 1 (2004).
[27] P. Ring and P. Schuck, *The Nuclear Many-Body Problem* (Springer-Verlag, New York, 1980), and references therein.
[28] R. Machleidt, Phys. Rev. C **63**, 024001 (2001).
[29] V. G. J. Stoks, R. A. M. Klomp, C. P. F. Terheggen, and J. J. de Swart, Phys. Rev. C **49**, 2950 (1994).
[30] D. R. Entem and R. Machleidt, Phys. Rev. C **68**, 041001(R) (2003).
[31] K. Suzuki and S. Y. Lee, Prog. Theor. Phys. **64**, 2091 (1980).
[32] F. Andreozzi, Phys. Rev. C **54**, 684 (1996).
[33] T. T. S. Kuo and Y. Tzeng, Int. J. Mod. Phys. E **3**, No. 2, 523 (1994).
[34] T. Hatsuda and S. H. Lee, Phys. Rev. C **46**, R34 (1992).
[35] M. Harada and K. Yamawaki, Phys. Rep. **381**, 1 (2003).
[36] F. Klingl, N. Kaiser, and W. Weise, Nucl. Phys. **A624**, 527 (1997).
[37] D. Trnka *et al.*, Phys. Rev. Lett. **94**, 192303 (2005).
[38] M. Naruki *et al.*, Phys. Rev. Lett. **96**, 092301 (2006).
[39] R. Rapp, R. Machleidt, J. W. Durso, and G. E. Brown, Phys. Rev. Lett. **82**, 1827 (1999).
[40] H. Müther and W. H. Dickhoff, Phys. Rev. C **72**, 054313 (2005).
[41] M. Baldo, I. Bombaci, and U. Lombardo, Phys. Lett. **B283**, 8 (1992).
[42] A. Schwenk, B. Friman, and G. E. Brown, Nucl. Phys. **A713**, 191 (2003).
[43] K. Hebeler, A. Schwenk, and B. Friman, Phys. Lett. **B648**, 176 (2007).